Acta Crystallographica Section B
Structural Science
ISSN 0108-7681

Synthesis and structural characteristics of lithocholate triads: steroid-type channels occupied by spacer fragments

Urszula Rychlewska,* Beata Warżajtis, Roman Joachimiak and Zdzisław Paryzek

Faculty of Chemistry, Adam Mickiewicz University, Poznań, Poland

Correspondence e-mail: urszular@amu.edu.pl

Received 28 February 2008
Accepted 7 March 2008

Reported in this paper are the syntheses and X-ray investigations of C_2 symmetrical molecular $A-B-A$ triads consisting of two steroid units (lithocholic acid or its methyl ester) joined together by linkers derived from bifunctional molecules such as terephthalic acid or *N*,*N*′-dicarboxypiperazine. Unlike their monomeric analogues, some of these compounds form inclusion complexes. All steroidal triads form crystals that are highly pseudo-centrosymmetric, in which the constituting molecules are held together either exclusively by van der Waals forces or form lattice inclusion complexes, with guest molecules hydrogen bonded to the host. The presence of carboxyl groups promotes the inclusion of pyridine molecules and the formation of the well known carboxylic acid···pyridine hydrogen bonds. Combined with pairwise face-to-face π-stacking between pyridine rings, these hydrogen-bond interactions lead to the formation of extended supramolecular tapes, analogous to polymers. The co-crystals of pyridine and a lithocholic acid triad undergo a symmetry-lowering phase transition from a *P*1 cell with $Z = 1$ to a *P*1 cell with $Z = 2$. The two structures are virtually the same, the two independent molecules in the larger cell being related by pseudo-translation. Changes in the type of spacer between two methyl lithocholate units from planar aromatic (terephthalic acid) to highly puckered aliphatic six-membered ring (*N*,*N*′-dicarboxypiperazine) bring about inclusion properties and changes in side-chain conformation in a crystal. Although the efficient packing of these highly elongated molecules is hindered, as indicated by low values of crystal density, ranging from 1.16 to 1.19 g cm^{-3}, several very short C···O and H···H contacts are present in the crystals.

1. Introduction

The molecules investigated belong to a broad group of molecular triads, $A-B-A$ (Gawroński & Kacprzak, 2002), in which the central unit *B* is a planar aromatic terephthalate or puckered heterocyclic piperazine-1,4-dicarboxylate, and *A* is derived from one of the steroidal bile acids, the lithocholic acid. The two *A* units are joined by the spacer group in a head-to-head (C3—C3) mode. In the field of steroids, a great diversity of dimeric and oligomeric structures has been reported, with the molecules of bile acids, or their derivatives, being linked by a spacer group in a head-to-head (C3—C3), head-to-tail (C3—C24) or tail-to-tail (C24—C24) fashion (Li & Dias, 1997*a*). Steroid triads exhibit micellar (Gouin & Zhu, 1998), liquid crystal (Hoffmann & Kumpf, 1986), catalytic (Guthrie *et al.*, 1986) and pharmacological (Pettit *et al.*, 1988, 1989) properties. They can act as artificial enzymes (Guthrie *et al.*, 1986), ion-transport devices (De Riccardis *et al.*, 2002;

Table 1
Experimental details.

	(5)·2Py (120 K)	(5)·2Py (180 K)	(6)	(7)·0.5MeOH
Crystal data				
Chemical formula	$C_{56}H_{82}O_8·2C_5H_5N$	$C_{56}H_{82}O_8·2C_5H_5N$	$C_{58}H_{86}O_8$	$C_{56}H_{90}N_2O_8·0.5CH_3OH$
M_r	1041.42	1041.42	911.27	935.32
Cell setting, space group	Triclinic, *P*1	Triclinic, *P*1	Monoclinic, *C*2	Triclinic, *P*1
Temperature (K)	120 (2)	180 (2)	293 (2)	130 (2)
a, *b*, *c* (Å)	12.8559 (6), 13.5462 (7), 17.4215 (9)	6.8044 (5), 12.8870 (9), 17.0661 (11)	31.731 (6), 7.727 (2), 11.017 (2)	7.7755 (9), 9.8697 (11), 17.754 (2)
α, β, gγ (°)	75.390 (4), 83.254 (4), 82.771 (4)	94.431 (6), 97.935 (6), 97.341 (5)	90.00, 106.28 (3), 90.00	103.040 (13), 101.086 (10), 90.463 (9)
V (Å^3)	2900.9 (3)	1463.14 (18)	2592.9 (10)	1300.7 (3)
Z	2	1	2	1
D_x (Mg m^{-3})	1.192	1.182	1.167	1.194
Radiation type	Mo $K\alpha$	Mo $K\alpha$	Cu $K\alpha$	Mo $K\alpha$
μ (mm^{-1})	0.08	0.08	0.59	0.08
Crystal form, colour	Plate, colourless	Plate, colourless	Needle, colourless	Plate, colourless
Crystal size (mm)	0.40 × 0.40 × 0.20	0.40 × 0.40 × 0.20	0.2 × 0.1 × 0.1	0.40 × 0.40 × 0.05
Data collection				
Diffractometer	Kuma KM4CCD κ geometry	Kuma KM4CCD κ geometry	KM-4 four circle	Kuma KM4CCD κ geometry
Data collection method	ω scans	ω scans	θ–2θ scans	ω scans
No. of measured, independent and observed reflections	22 008, 10 239, 6040	11 263, 5162, 3150	4425, 2419, 715	10 039, 4568, 2473
Criterion for observed reflections	$I > 2\sigma(I)$	$I > 2\sigma(I)$	$I > 2\sigma(I)$	$I > 2\sigma(I)$
R_{int}	0.069	0.037	0.196	0.052
θ_{max} (°)	25.1	25.1	65.8	25.1
Refinement				
Refinement on	F^2	F^2	F^2	F^2
$R[F^2 > 2\sigma(F^2)]$, $wR(F^2)$, S	0.078, 0.146, 1.02	0.050, 0.124, 0.93	0.046, 0.137, 0.86	0.070, 0.159, 0.98
No. of reflections	10 239	5162	2419	4568
No. of parameters	1381	673	299	619
H-atom treatment	Riding	Riding	Riding	Riding
Weighting scheme	$w = 1/[\sigma^2(F_o^2) + (0.042P)^2]$, where $P = (F_o^2 + 2F_c^2)/3$	$w = 1/[\sigma^2(F_o^2) + (0.066P)^2]$, where $P = (F_o^2 + 2F_c^2)/3$	$w = 1/[\sigma^2(F_o^2) + (0.0586P)^2]$, where $P = (F_o^2 + 2F_c^2)/3$	$w = 1/[\sigma^2(F_o^2) + (0.0706P)^2]$, where $P = (F_o^2 + 2F_c^2)/3$
$(\Delta/\sigma)_{max}$	0.009	< 0.0001	< 0.0001	< 0.0001
$\Delta\rho_{max}$, $\Delta\rho_{min}$ (e Å^{-3})	0.21, −0.19	0.20, −0.18	0.20, −0.14	0.29, −0.22
Extinction method	None	None	*SHELXL*	None
Extinction coefficient	–	–	0.00071 (11)	–

Computer programs: *CrysAlis CCD* (Oxford Diffraction, 2001*a*, 2004*a*), *KM*4 software (Kuma Diffraction, 1995), *CrysAlis RED* (Oxford Diffraction, 2001*b*, 2004*b*), *SHELXS*86 (Sheldrick, 1990), *SHELXL*97 (Sheldrick, 2008), Siemens (1989), *Mercury* (Bruno *et al.*, 2002).

Goto *et al.*, 2001; Kobuke & Nagatani, 2001) and have been used as structural components in molecular engineering (Davis, 1993). Hoffmann & Kumpf (1986) reported the synthesis of estrone triads. The natural dimeric steroid pyrazine alkaloids, cephalostatins, possess cell-growth inhibition activity (Pettit *et al.*, 1988, 1989). These compounds have been isolated from marine worms and their structure has been assigned on the basis of NMR and mass spectral analysis (Pettit *et al.*, 1988, 1989). Oligomerization of steroids can lead to new biologically active compounds (Salunke *et al.*, 2004; Yoshimura *et al.*, 2001). These steroidal dimers are also potential substrates for the synthesis of macrocyclic compounds having artificial receptor properties (Davis, 1993; Evans *et al.*, 1995; Bhattarai *et al.*, 1997; Tamminen & Kolehmainen, 2001). In the synthesis of steroidal triads a variety of spacer groups as steroid linkers have been proposed (Li & Dias, 1997*a*; Davis, 1993; Tamminen & Kolehmainen, 2001). Recently, the synthesis of a tail-to-tail triad of (20*S*)-5α-23,24-bisnorchol-16-en-3β,6α,7β,22-tetrol derivative with the terephthalate linker has been presented by Di Filippo and co-workers (Di Filippo *et al.*, 2003). The triad compound was active as a Na^+-transporting trans-membrane channel (De Riccardis *et al.*, 2002). Among steroids, bile acids are the most frequently used for the synthesis of dimeric and oligomeric artificial receptors. The amphiphilic properties, the well defined geometry and availability are the main features that make bile acids excellent building blocks in the synthesis of the supramolecular hosts (Tamminen & Kolehmainen, 2001; Bonar-Law & Davis, 1993*a*,*b*; Bonar-Law *et al.*, 1993). Davies and co-workers presented the synthesis and a spectral study of cholaphane, the first bile-acid-based macrocyclic compound (Bonar-Law & Davis, 1993*a*,*b*; Bonar-Law *et al.*, 1993) acting as an artificial receptor for glucosides (Bhattarai *et al.*, 1997). In 2003, Nahar and Turner presented the synthesis of a new lithocholic acid triad of the head-to-tail type (Nahar & Turner, 2003). The effective coupling of the lithocholic and cholic acid residues by the terephthalate linker to give a C3—C3 triad has been reported (Joachimiak & Paryzek, 2004). The compounds

showed alkaline metal-ion binding ability. Another example of cyclic head-to-tail dimers with no spacer group are the cyclocholates (Li & Dias, 1997*a*).

Here we report the crystal structures of new head-to-head bile acid triads (5), (6) and (7), in which a diester [(5) and (6)] or diurethane linkage (7) between C3 positions of two lithocholic acid [3α-hydroxy-5β-cholan-24-oic acid (1)] or methyl lithocholate molecules (2) is present. While the synthesis of (6) has been described in our earlier report (Joachimiak & Paryzek, 2004), the synthetic procedure for (5) and (7), including intermediate products (4) and (8), is presented in this paper.

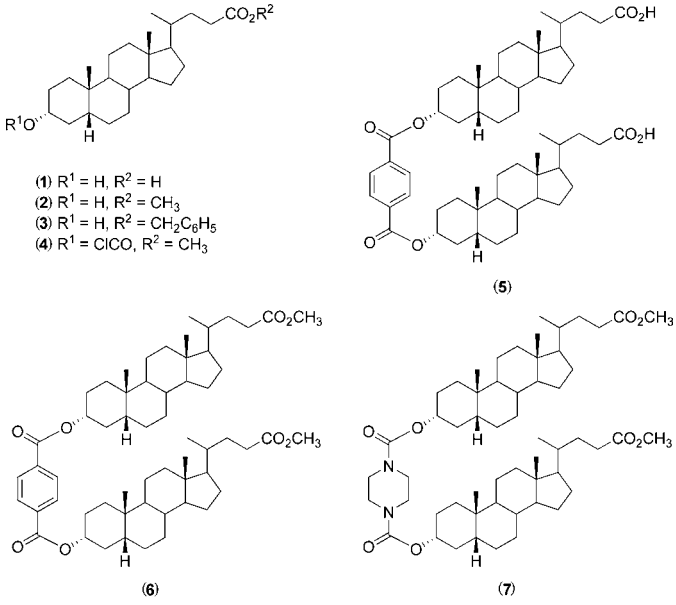

2. Experimental

2.1. Physicochemical measurements

M.p. values were determined on a Kofler hot-stage apparatus and are uncorrected. IR spectra were determinated with a FT-IR Bruker FS 113V spectrophotometer. ^{1}H and ^{13}C NMR spectra were recorded with a Varian Gemini 300 VT spectrometer operating in the Fourier transform mode. Chemical shifts (δ) are expressed in p.p.m. relative to tetramethylsilane as the internal standard. The DEPT technique was used for the assignment of multiplicity of carbon signals in ^{13}C NMR spectra. The additivity rules and comparison with data reported for compounds of similar structure were helpful for signal assignment. Electrospray mass spectra experiments were performed using a Waters/Micromass ZQ ES mass spectrometer with a methanol solvent system entering the chamber at a rate of 40 ml min^{-1}. The source temperature was 393 K and the cone voltage was set at 30 V. Solvents were dried and distilled according to the standard procedures. Reaction progress and the purity of the compounds was monitored by TLC using precoated aluminium-backed silica plates (Merck, No. 5554). Silica gel 60 (Merck 70-230 mesh, No. 7734) was used for flash chromatography. The thermal stability has been evaluated by thermogravimetric analysis (TG-DTA).[1]

2.2. X-ray measurements

Crystal data, data collection and refinement parameters for (5)·2Py (measured at two different temperatures), (6) and (7)·0.5MeOH are summarized in Table 1. Reflection intensities for (6) were measured at room temperature on a four-circle KM-4 Kuma Diffraction diffractometer (Kuma Diffraction, 1995) using graphite-monochromated Cu $K\alpha$ radiation (λ = 1.54178 Å) and those for (5)·2Py and (7)·0.5MeOH were collected on a KM4CCD diffractometer (Oxford Diffraction, 2001*a*, 2004*a*) using graphite-monochromated Mo $K\alpha$ radiation (λ = 0.71073 Å) at 120 and 180 K for (5)·2Py, and 130 K for (7)·0.5MeOH. The low temperature was controlled with an Oxford Instruments cryosystem cooling device. During the process of lowering the temperature of the crystals of (5)·2Py we started to see additional reflections corresponding to a larger unit cell. X-ray data for this cell have been measured at 120 K. Subsequently, we started to gradually raise the temperature, while still collecting and visually inspecting the diffraction images in order to precisely determine the temperature of the phase transition. However, we have not succeeded in this, presumably because the phase transition took place gradually over a wide temperature range. The crystals decomposed in air, therefore repetition of the experiment was not possible without obtaining a new sample. At a temperature of 180 K no reflections corresponding to the larger cell were present on the diffraction images, so the data collection procedure was repeated. The two sets of data represent two crystal structures of (5)·2Py, both triclinic, space group $P1$, which differ in the number of independent molecules in the unit cell: $Z = 2$ and $Z = 1$, respectively. Both crystal structures contain pyridine solvent molecules in a host-to-guest ratio of 1:2. Phase transitions that occur during cooling and that are associated with an integral multiplication of the unit-cell volume are relatively common (Xia *et al.*, 2001). In the case in question the doubling of the unit-cell volume is a direct result of doubling the a axis in (5)·2Py (180 K) to generate the b axis in (5)·2Py (120 K).

The structures were solved by direct methods using *SHELXS*86 (Sheldrick, 2008) and refined by least-squares refinements on F^2, applying the *SHELXL*97 (Sheldrick, 2008) system of programs. The intensity data were corrected for Lp effects. Anisotropic displacement parameters were employed for the non-H atoms. The positions of the C—H hydrogen atoms were calculated at standardized distances of 0.96 Å [0.98 Å for methyl groups in (5)·2Py and (7)·0.5MeOH], except for the O—H hydrogen atoms, which were located on difference-Fourier maps. All H atoms (including those located on the difference-Fourier maps) were refined using a riding model, *i.e.* the H atoms were allowed to move simultaneously

[1] Supplementary data for this paper, including the synthesis details, the NMR, IR and mass spectrometry results for (4), (5), (7) and (8), and the TG-DTA diagram of the 1:2 complex of (5) with pyridine, are available from the IUCr electronic archives (Reference: BK5073). Services for accessing these data are described at the back of the journal.

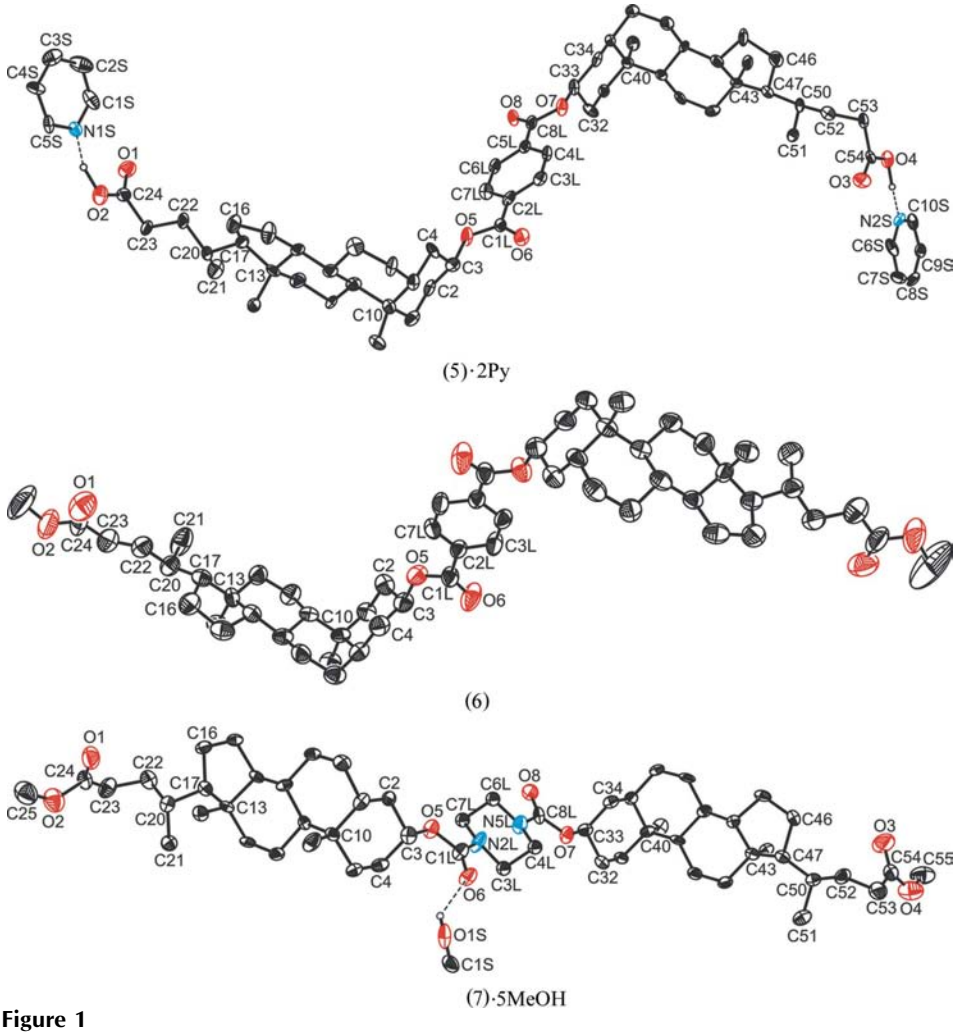

Figure 1
Perspective view of the investigated steroidal triads with solvent molecules hydrogen bonded to the hosts. H atoms not participating in hydrogen bonds have been omitted for clarity. The labelling scheme shown was used consistently for all the molecules studied. In the disordered molecule (7) only one of two alternative orientations is shown. Displacement ellipsoids are drawn at the 40% probability level.

with the atoms to which they were attached, keeping the bond lengths and angles constant, and their isotropic displacement parameters were given a value 20% higher than the isotropic equivalent for the atom to which the H atom was bonded. In the low-temperature structure of (5)·2Py the 25 atoms that were nearly non-positive-definite (NPD) were refined using the ISOR instruction which restrains the U^{ij} components of anisotropically refined atoms to behave approximately isotropically. The elongated shape of the ellipsoids in the higher-temperature structure of (5)·2Py indicated possible disorder of some parts of the molecule. This has been accounted for by assuming that the atoms C11, C12, C18, C19, C21, C35, C36, C37, C38, C44, C45 and C46 equally occupy two position sites (their equivalents at the other site were designated with primes). The atoms engaged in the disorder were refined isotropically because of the limited number of observations. The two equally occupied sites mirror a superposition of the two crystallographically different molecules in the structure (5)·2Py (120 K). Also, in the crystal structure of (7)·0.5MeOH the piperazine C atoms (C2, C3, C5, C6) were found to be disordered over two alternative orientations. The piperazine disorder was modelled in an analogous manner, *i.e.* in the form of unprimed and primed component with equal occupancy. The disordered atoms were refined isotropically. The absolute structure of the crystals was assumed from the known absolute configuration of lithocholic acid used as the starting material in the synthesis. Structures were viewed and analysed, and drawings were prepared with *Mercury* (Bruno *et al.*, 2002) and Siemens computer graphics (Siemens, 1989) programs.

3. Results and discussion

3.1. Synthesis

The ester-linked triad (5) was synthesized from lithocholic acid (1) in three steps, as shown below.

In the first step, the carboxyl group of lithocholic acid (1) was protected as the corresponding benzyl ester *via* reaction with benzyl alcohol by using 1,3-dicyclohexyl carbodiimide (DCC) and 4-dimethylaminopyridine (DMAP) to give (3) (Li & Dias, 1997*b*). The reaction of (3) with terephthaloyl chloride in anhydrous benzene afforded (8) in 74% yield after chromatography. Hydrogenolysis of the benzyl ester (8) with ammonium formate as a hydrogen donor and 10% palladium on carbon as a catalyst in methanol solution (Paryzek *et al.*, 2003) gave the diacid triad (5) in quantitative yield. The hydrogen-bonded complex of triad (5) with pyridine was obtained upon crystallization of (5) from pyridine.

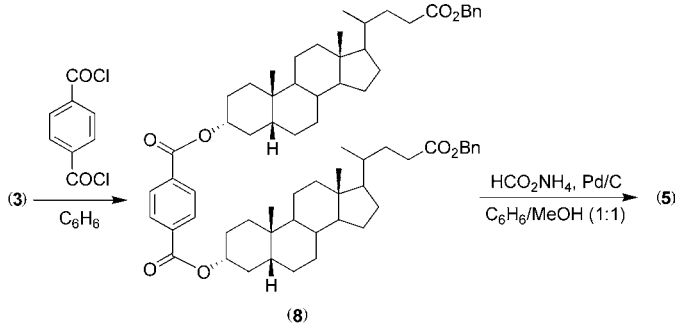

Compound (6) (Joachimiak & Paryzek, 2004) was crystallized from 1,4-dioxane.

The diurethane linkage in (7) was obtained from methyl lithocholate (2) (Dayal *et al.*, 1981), as shown below. The

Table 2
Torsion angles (°) describing the conformation of the side chain and the mutual orientation of steroid and linker fragments.

	(5) (120 K)	(5′) (120 K)	(5) (180 K)	(6)	(7)†
C16—C17—C20—C22 (φ_1)	57.6 (8)	57.7 (8)	56.7 (6)	60.7 (9)	51.3 (8)
C46—C47—C50—C52 (φ_1)	58.8 (8)	57.3 (8)	69.6 (6)	60.7 (9)	55.6 (7)
			46.3 (7)‡		
C17—C20—C22—C23 (φ_2)	−175.9 (6)	−180.0 (6)	−177.6 (5)	−170.1 (7)	−166.5 (6)
C47—C50—C52—C53 (φ_2)	−169.7 (6)	−173.6 (6)	−172.6 (4)	−170.1 (7)	−164.6 (6)
C20—C22—C23—C24 (φ_3)	167.2 (7)	158.4 (7)	162.2 (5)	−179.0 (10)	64.7(9)
C50—C52—C53—C54 (φ_3)	−93.7 (8)	−94.1 (8)	−92.7 (6)	−179.0 (10)	60.4 (9)
C22—C23—C24—O2 (φ_4)	−93.0 (8)	−99.9 (8)	−96.3 (6)	−164.2 (10)	−153.0 (7)
C52—C53—C54—O4 (φ_4)	144.9 (7)	143.5 (7)	143.2 (4)	−164.2 (10)	−154.1 (8)
C1*L*—O5—C3—C2	−140.5 (7)	−160.7 (6)	−151.9 (4)	−132.1 (8)	−85.5 (7)
C1*L*—O5—C3—C4	95.5 (8)	81.0 (7)	87.3 (5)	107.3 (9)	156.2 (6)
C8*L*—O7—C33—C32	−84.0 (8)	−107.7 (8)	−93.2 (5)	−132.1 (8)	−151.4 (6)
C8*L*—O7—C33—C34	152.4 (6)	135.6 (7)	146.4 (5)	107.3 (9)	85.9 (7)
O6—C1*L*—O5—C3	0.3 (11)	8.0 (10)	3.8 (8)	6.9 (17)	3.5 (11)
O8—C8*L*—O7—C33	−8.9 (11)	2.6 (12)	−5.4 (8)	6.9 (17)	−5.9 (11)
C3*L*—C2*L*—C1*L*—O6	−16.9 (11)	1.2 (11)	−4.5 (8)	7.2 (16)	15.1 (13)
					−21.4 (13)‡
C7*L*—C2*L*—C1*L*—O6	166.9 (7)	−176.8 (7)	175.4 (5)	−171.4 (12)	157.0 (11)
					−167.0 (11)‡
C4*L*—C5*L*—C8*L*—O8	179.0 (7)	−167.1 (8)	−175.7 (5)	7.2 (16)	−163.3 (10)
					166.0 (10)‡
C6*L*—C5*L*—C8*L*—O8	4.2 (11)	10.4 (12)	5.7 (8)	−171.4 (12)	−18.6 (12)
					16.8 (13)‡

† C2*L* and C5*L* become N2*L* and N5*L*, respectively. ‡ Values corresponding to the second component of disorder.

The stereochemistry of the basic steroid skeleton can be described as *cis-anti-trans-anti-trans*.[2] All the six-membered rings *A*, *B* and *C* adopt almost perfect chair conformations and the five-membered *D* ring displays either a C13-envelope, C13—C14 twist or mixed envelope/twist conformation. Finding a correlation between the side chain and the D-ring conformations, as suggested by Giglio (1984), is not straightforward. The side-chain conformation can be described by a set of four torsion angles φ_1–φ_4 (Giglio & Quagliata, 1975) that are reported in Table 2. The values of φ_1 and φ_2 are the same in all the molecules studied and are *ca* 60 and −170°, respectively, while φ_3 adopts values around 170 (*trans*), −90 and 60° (*gauche*), and φ_4 adopts values around −160 (*trans*), −95 (*gauche*) and 144° (*anti*). The quoted range of data illustrates that the side chain in these molecular triads displays substantial conformational flexibility, but conformational changes are restricted to only two torsion angles, φ_3 and φ_4. The most extended side-chain conformation is present in molecule (6), consisting of two methyl lithocholate residues connected by a terephthalate spacer. The side-chain conformation in this crystal structure can be described as *gauche-trans-trans-trans* (Table 2). The molecule of (6) retains its twofold symmetry in a crystal, while (7), which differs from (6) in the type of spacer molecule (piperazine-1,4-dicarboxylate instead of terephthalate), displays only approximate C_2 symmetry, and adopts a *gauche-trans-gauche-trans* conformation of the side chain, the same at both ends of the molecule. Unlike (6) and (7), where the side chain is not engaged in specific intermolecular interactions, (5) contains free carboxyl groups, ready to be involved in hydrogen-bond interactions. The compound crystallizes exclusively from pyridine solution and forms two types of crystals depending on the temperature (above or below 180 K). Both high- and low-temperature phases are triclinic, space group *P*1, and differ mostly in that the unit-cell volume of the low-temperature phase is doubled, leading to an increase of *Z* (*i.e.* the number of molecules in the unit cell) from 1 to 2. The two independent molecules of (5) present in the low-temperature form as well as the disordered molecule forming the high-temperature crystal structure are very much alike; all are asymmetric (C_1 symmetry) and display different side-chain conformations at the two ends of the molecule (*gauche-trans-trans-gauche versus gauche-trans-gauche-anti*, Table 2). Taking into account that (5) crystallizes

reaction of (2) with phosgene, generated from triphosgene, afforded the 3-chloroformyl derivative (4) which upon reaction with piperazine in tetrahydrofuran in the presence of 4-dimethylaminopyridine (DMAP) gave (7), which was crystallized from the 4:1 mixture of $CHCl_3$ and CH_3OH to give solvated crystals of (7)·0.5MeOH.

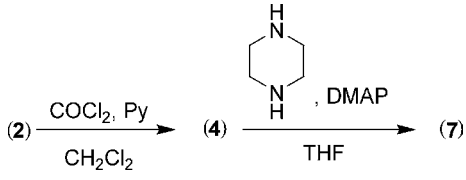

3.2. Molecular conformation and disorder

Fig. 1 shows a perspective view of molecules (5), (6) and (7), as found in the crystal lattice. Compounds (5) and (7) crystallize with solvent molecules with a host-to-guest ratio of 1:2 and 2:1, respectively. The investigated molecules belong to a group of steroidal *A*—*B*—*A* triads (formed by either lithocholic acid or its methyl ester) linked by a planar aromatic terephthalate or puckered heterocyclic piperazine-1,4-dicarboxylate spacer. Hence, each molecule has a potential C_2 molecular symmetry and can adopt either an extended (Z-shaped) or a folded (C-shaped) conformation, depending whether the steroidal fragments are located on the opposite or the same face of the linker. It appears that in a crystal all investigated molecules form the extended and highly puckered *Z* conformations (Fig. 1).

[2] The descriptors ('*trans*' and '*cis*') are used for decalin-like junctures, whereas the descriptors '*anti*' are used for two adjacent ring junctures to the central ring involving the two peripheral rings. The alternative descriptor for '*anti*' is '*transoid*'.

with pyridine solvent molecules by forming strong carboxylic acid···pyridine hydrogen bonds (see §3) we may assume that we witness the guest-induced conformational changes in the molecules of (5), which mostly affect the φ_3 and φ_4 torsion angles, *i.e.* the shape of the side chain and orientation of the carboxyl groups.

Another source of molecular flexibility is the presence of a conformationally labile spacer, linking two steroidal fragments *via* ester or carbamate bonds. Mutual arrangement of the steroid and spacer units in a triad can be described by a set of torsion angles around $C^*_{steroid}-O$, $O-C_{carb}$ and $C_{carb}-C(or\ N)_{linker}$ bonds (where carb is carbonyl). This set of values, listed in Table 2, illustrates that the orientation of the spacer with respect to the two steroid moieties differs moderately in molecules (5) and (6), but significantly in (7), containing the disordered piperazine linker. The disorder model points to the existence of two sites, equally occupied by highly puckered piperazine rings in, respectively, chair and inverted chair conformations, and with N atoms in fixed positions. Cremer and Pople parameters for the two piperazine rings are: QT = 0.70 (1) and 0.56 (1) Å; $\theta = 176$ (1) and 1 (1)°; $\varphi = 164$ (16) and −102 (43)°, for unprimed and primed piperazine rings, respectively. The two independent molecules of (5) (120 K) differ somewhat in rotation around all bonds describing the orientation of the terephthalate moiety with respect to the steroid residues, particularly in the degree of planarity of the terephthalate fragments, while the molecule of (5) (180 K) displays values intermediate between the two sets. The degree of co-planarity of the two terephthalate carbonyl groups with the benzene ring is different in each molecule, except for the symmetrical molecule (6).

3.3. Crystal packing, inclusion properties and intermolecular interactions

The arrangement of molecules viewed along the shortest crystallographic axis is illustrated in Figs. 2, 3 and 4. The wavy Z-shape of the triads combined with the triclinic lattice [in the crystals of (5) and (7)] assures that a single lattice translation is sufficient to shift one molecule with respect to the other by half of its length, width and thickness (for the definition of molecular dimensions see Duax & Norton, 1975). Although the molecules lack many of the characteristics of bile acids, they pack in a way resembling the bilayer packing of the cholic acids (Hishkawa *et al.*, 1998). The analogy can be visualized if, for the sake of comparison, the presence of a spacer is neglected. This is illustrated in Figs. 3 and 4, where a single triad molecule participates in the formation of the first and fourth steroidal sheet with parts of two other molecules sandwiched in between. It can be seen from these figures that in the investigated crystal structures the spacer fragments situate themselves in the area reserved for guest molecules in bile acid clathrates, *i.e.* in grooves formed between the corrugated host bilayers. Moreover, solvent molecules present in the crystal structures of (5) and (7) also occupy this region, as depicted by the enlarged area in Figs. 2 and 4. The bottom part of Fig. 2, designed to illustrate the analogy of the host framework in (5) with the bile acid clathrates, shows the arrangement of methyl groups within the hydrophobic region and *trans*, *gauche* conformation of the steroidal side chains around the C22—C23 and C52—C53 bonds. The investigated steroidal triads lack the hydrogen-bond potential characteristic for bile acids, where the association is driven by OH···OH hydrogen bonds. Nevertheless, in their crystal structures we observe hydrogen bonds resulting from host/guest interactions. Inclusion-forming properties have been

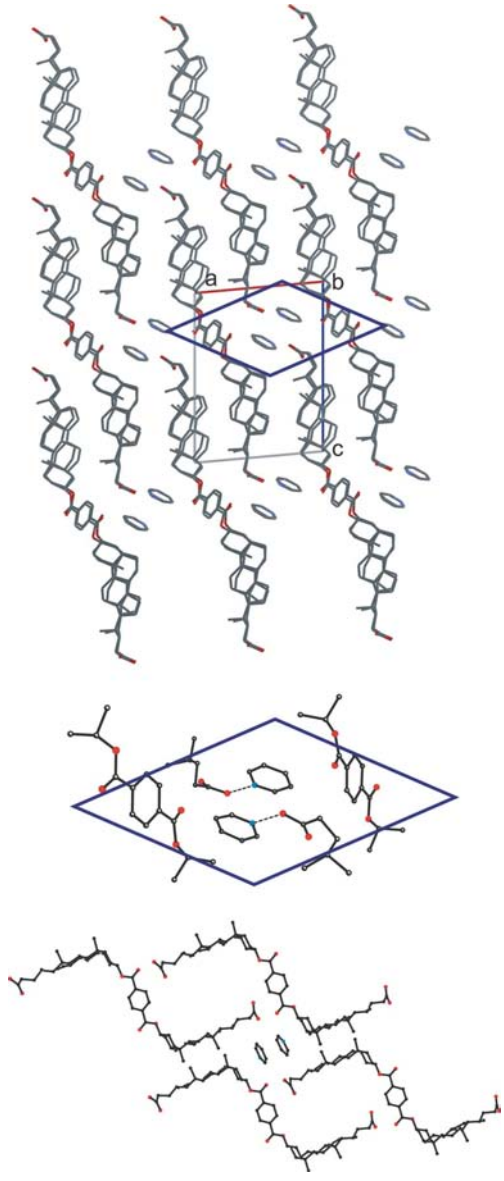

Figure 2
View along [010] of the crystal structure at 120 K of (5)·2Py. Molecules from the neighbouring (010) layers are related by pseudotranslation. Packing in the crystal structure determined at 180 K is nearly identical except for the symmetry increase from pseudo- to true lattice translation. The highlighted area illustrates the solvent channel propagating along the [010] direction with pyridine molecules engaged in pairwise face-to-face π-stacking interactions and the spacer fragments. (bottom) Side view illustrating the resemblance of the observed pyridine channel to the *trans-gauche* type of the solvent channels formed by some bile-acid hosts.

Table 3
Hydrogen-bond parameters (Å, °).

	D—H (Å)	*D*···*A* (Å)	H···*A* (Å)	*D*—H···*A* (°)
(5) (120 K)				
O2—H2O···N1*S*	1.20	2.618 (9)	1.47	160
O4—H4O···N2*S*	1.19	2.654 (9)	1.47	176
O2′—H2′O···N3*S*	1.15	2.617 (10)	1.50	162
O4′—H4′O···N4*S*	1.28	2.611 (9)	1.41	152
C3—H3···O6	0.96	2.731 (10)	2.38	101
C52—H52*A*···O3	0.96	2.978 (9)	2.59	104
C33′—H33′···O8′	0.96	2.705 (10)	2.33	103
C52′—H52*C*···O3′	0.96	2.959 (9)	2.55	106
C2*S*—H2*S*···O2′^{i}	0.96	3.307 (10)	2.56	135
C53—H53*A*···O8′^{ii}	0.96	3.344 (10)	2.46	154
C3*L*—H3*L*···O1′^{ii}	0.96	3.296 (9)	2.50	140
C53′—H53*C*···O8^{iii}	0.96	3.393 (9)	2.56	145
C13*S*—H13*S*···O8^{iv}	0.96	3.592 (12)	2.63	179
C17*S*—H17*S*···O4^{v}	0.96	3.278 (10)	2.59	128
(5) (180 K)				
O2—H2O···N1*S*	1.24	2.618 (7)	1.39	170
O4—H4O···N2*S*	1.31	2.640 (6)	1.34	171
C33—H33···O8	0.96	2.700 (6)	2.35	101
C52—H52*A*···O3	0.96	2.976 (7)	2.58	105
C2*S*—H2*S*···O2^{vi}	0.96	3.330 (8)	2.63	130
C53—H53*B*···O8^{v}	0.96	3.385 (6)	2.53	148
C3*L*—H3*L*···O1^{v}	0.96	3.388 (6)	2.63	137
(6)				
C3—H3···O6	0.96	2.713 (10)	2.32	104
C3*L*—H3*L*···O6	0.96	2.851 (11)	2.50	102
C3—H3*G*···O6^{vii}	0.96	3.478 (8)	2.59	155
(7)				
O1*S*—H1*SG*···O6	0.84	2.819 (13)	2.15	136
C50—H50···O3	0.96	3.207 (10)	2.61	120
C3*L*—H3*LB*···O6	0.96	2.751 (13)	2.37	103
C3*L*′—H3*LC*···O6	0.96	2.733 (13)	2.38	101
C4*L*—H4*LB*···O7	0.96	2.669 (14)	2.29	103
C4*L*′—H4*LC*···O7	0.96	2.634 (13)	2.27	101
C6*L*—H6*LB*···O8	0.96	2.794 (13)	2.44	102
C6*L*′—H6*LC*···O8	0.96	2.738 (14)	2.36	103
C7*L*—H7*LA*···O5	0.96	2.728 (15)	2.34	103
C7*L*′—H7*LD*···O5	0.96	2.705 (14)	2.38	99
C3—H3···O8^{viii}	0.96	3.378 (10)	2.44	167
C33—H33···O6^{ii}	0.96	3.512 (10)	2.57	168
C6*L*′—H6*LD*···O3^{ix}	0.96	3.475 (18)	2.58	154
C7*LG*—H7*LB*···O3^{ix}	0.96	3.019 (19)	2.12	156
C4*L*′—H4*LC*···O1^{x}	0.96	3.022 (16)	2.59	108
C4*L*—H4*LB*···O1^{x}	0.96	3.298 (16)	2.66	125
C3*L*—H3*LB*···O1^{x}	0.96	3.156 (13)	2.67	112
C3*L*′—H3*LD*···O2^{xi}	0.96	3.473 (17)	2.64	146
C6*L*—H6*LA*···O2^{xi}	0.96	3.285 (17)	2.42	150
C4*L*—H4*LA*···O2^{xi}	0.96	3.318 (18)	2.47	148
C7*L*′—H7*LC*···O2^{xi}	0.96	3.494 (18)	2.63	150
C7*L*′—H7*LC*···O4^{xii}	0.96	3.205 (16)	2.67	116
C6*L*—H6*LA*···O4^{xii}	0.96	2.963 (15)	2.50	110

Symmetry codes: (i) $x, y, z+1$; (ii) $x, y+1, z$; (iii) $x, y, z-2$; (iv) $x-1, y-1, z$; (v) $x, y, z-1$; (vi) $x-1, y, z$; (vii) $-x, y, -z$; (viii) $x, y-1, z$; (ix) $x, y-1, z-1$; (x) $x+1, y+1, z+1$; (xi) $x, y+1, z+1$; (xii) $x-1, y-1, z-1$.

observed in crystals of (5) (pyridine) and (7) (methanol), but not in (6). The hydrogen-bond parameters, including numerous C—H···O interactions, are listed in Table 3.

Compound (5), being hardly soluble in any common organic solvent, crystallizes from pyridine with a host:guest ratio of 1:2 giving rise to strong O—H···N(pyridine) hydrogen bonds often employed in the construction of extended architectures in the solid state (Aakeröy *et al.*, 2005; Aakeröy *et al.*, 2007; Babu & Nangia, 2006; Vishweshwar *et al.*, 2002). Our recent CSD search (Allen, 2002) revealed that although both O—H···N and N^{+}—H···O^{-} hydrogen bonds are possible, the former is reported 228 times, while the latter only 97 times. Geometrical parameters describing hydrogen-bond interactions are similar for the two types of bonds, although a slight tendency for uncharged hydrogen bonds to form shorter bonds is noticeable [average H···N distances are 1.70 (1) Å, as opposed to 1.76 (2) Å]. In the investigated crystal structures both the H···N and O···N distances are much shorter than the quoted mean values, giving average values of 1.46 (3) and

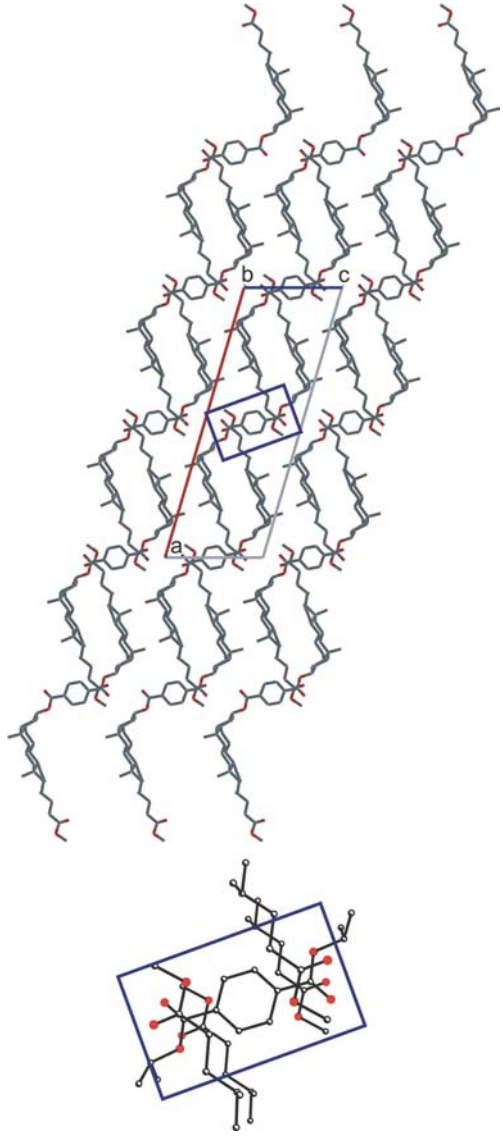

Figure 3
Packing of molecules of (6), as viewed along the twofold axis (b = 7.727 Å). Steroid triads are disposed around the twofold axis and are arranged in (010) layers, with molecules in the neighbouring layers shifted by approximately half of the unit translation in both the a and c directions. The figure is a projection of two consecutive layers. All ester groups, either constituting the side chain or the linker, are concentrated in the same region, *i.e.* around lattice points 0, y, $\frac{1}{2}$ and $\frac{1}{2}$, $\frac{1}{2}+y$, $\frac{1}{2}$ (highlighted area).

2.63 (3) Å at 120 K, and 1.38 (1) and 2.63 (2) Å at 180 K. The shortest and the longest of these bonds correspond, respectively, to the least and the most linear hydrogen bond. Detailed analysis of hydrogen-bond parameters listed in Table 3 reveals contraction of some of the O···N and H···N distances and accompanied lengthening of O—H bonds. This might indicate that at least in some of these hydrogen bonds partial proton transfer takes place, *i.e.* the proton is shared to form very strong intermolecular hydrogen bonds. The presence of the accompanying $C-H_{pyr}\cdots O{=}C$ (where pyr is pyridine) hydrogen-bond interactions, which would close the $R_2^2(7)$ motif has been ruled out on the basis of geometrical considerations. The structure is additionally stabilized by pairwise face-to-face π-stacking interactions between pyridine rings which are oriented mutually antiparallel. The two interacting pyridine rings are inclined at angles not exceeding 3.7 (6)°, and with the center-to-center distances in the range from 3.641 (7) to 3.670 (7) Å, and with a perpendicular distance between rings in the range 3.303 (7)–3.414 (7) Å. Judging from these parameters, the stacking interactions are strong, and a combination of strong O—H···N hydrogen bonds with π-stacking interactions leads to the formation of corrugated supramolecular tapes, passing through the entire crystal. To the best of our knowledge, this crystal structure constitutes the first example of the infinite tape motifs formed by a steroidal carboxylic acid/pyridine complex. Dihedral angles between pyridine and carboxylate groups are consistently larger for the side chain in the *trans-gauche* conformation [average value 21 (1)°], than in the *gauche-anti* conformation [average value 3.0 (8)°]. Pyridine molecules are arranged in pairs, and are situated in channels that propagate along the *b* direction (Fig. 2). Adapting a notation used to describe the various types of channels formed by the bile acid crystals (Miyata & Sada, 1996), we can describe the pyridine channels as of the *trans-gauche* type (see the bottom part of Fig. 2). It might be worth mentioning that the classical steroidal channels are usually constructed from molecules with their side chains in either exclusively *gauche* or *trans* conformations. Asymmetrical, *trans-gauche* combinations are very rare and, if present, might lead to the closure of the channels (Hishikawa *et al.* 1998), although a more recent report points to their presence in the crystal structure of 2:1 cholic acid–benzophenone clathrate (Nowak *et al.*, 2000). Inclusion properties of (5) and asymmetry in its side-chain conformation most probably originate from the preference of this steroidal triad to form hetero- rather than homomolecular associations, which assures more dense packing, and antiparallel arrangement of host molecules in a channel.

The C-centred monoclinic lattice of (6) contains only two molecules, arranged around twofold axes and packed in (010) layers. The molecules in neighbouring layers are shifted approximately by half of the unit translation along the **a** and **c** directions, giving rise to a double-layer arrangement along the twofold *b* axis. The packing diagram along this direction, shown in Fig. 3, closely resembles the side view of the double-layer arrangement of bile acids. The crystal of (6) does not show any inclusion, like its parent compound, methyl lithocholate (2) (Virtanen *et al.*, 2003), which also forms guest-free crystals. However, as can be seen from Fig. 3, the space occupied by the terephthalate linker corresponds to this region in bile acids clathrates, where the grooves created by hydrophobic pleated sheets are situated, thus enhancing the striking similarity between the packing mode of bile acid inclusion compounds and the steroidal triad (6). Unlike (6), the crystal structure of (7)·0.5MeOH is extended exclusively by lattice translations. The molecules pack in the (100) layer (Fig. 4). Changes in the type of linker from planar aromatic to chair-type heterocyclic induce changes in the side-chain conformation at both ends of the molecule from *trans* to *gauche* (around C22–C23 and C52–C53). As in (6), the side chains in the crystals of (7)·0.5MeOH are situated in the same region as the linker but, owing to the folding caused by the *gauche* conformation, they embrace the linker instead of extending over it. Folding of the side chain prevents the

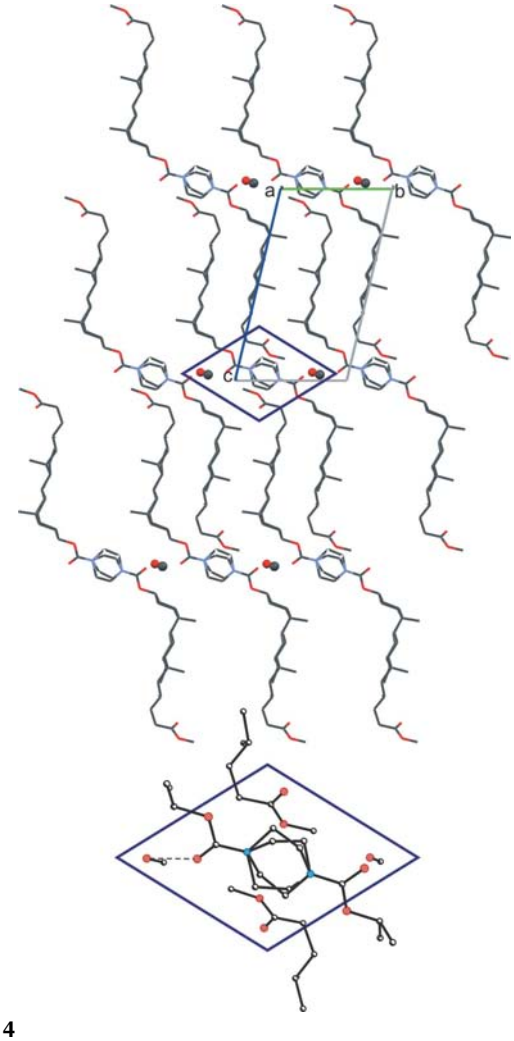

Figure 4
Packing of molecules of (7) as viewed along the shortest axis (a = 7.776 Å) displays one highly corrugated (100) layer. A single steroid molecule extends from the first to the fourth (010) level with parts of two other molecules sandwiched in between. The highlighted area illustrates the concentration of spacer fragments (disordered over two sites), side-chain ester functions, and methanol solvent molecules in one region of space.

formation of unavoidable short contacts with the highly puckered piperazine ring that would occur if the chains were in all *trans* conformations. Most likely this obstacle has not been fully overcome giving rise to an extended list of short C—H···O interactions (Table 3) and to the disorder of the piperazine ring. Compound (7) crystallizes with methanol solvent molecules in a 2:1 ratio. The solvent molecules are situated in close proximity to the spacer carbamate moiety and are hydrogen bonded to the linker O6 carbonyl oxygen (Table 3). They also form an extremely short contact with the terminal methyl ester group, the Csp^3···O1S distance being only 2.87 (1) Å. In the crystal structure of (7)·0.5MeOH short contacts are also seen between the methyl ester O atoms and the distorted parts of the piperazine linker, and appear as a result of an embrace of the piperazine ring by the folded side chains.

The type of packing observed in the crystal structures of (6) and (7)·0.5MeOH promotes dual hydrogen-bond association *via* C3—$H_{steroid}$···O=C_{linker} hydrogen bonds (Table 3) and generation of the corresponding $R_2^2(10)$ hydrogen-bond motifs. The motifs link molecules related by either a twofold symmetry axis (6) or by a single lattice translation [(7)·0.5MeOH] and are formed at both sides of the spacer in the region where the hydrophilic interactions operate. Additional stabilization of the described hydrogen-bond motif comes from the intramolecular interactions operating between antiparallel local 1,3-CH/CO dipoles (Rychlewska & Warżajtis, 2000) formed along C3—$H_{steroid}$/C1*L*=O6 and C33—$H_{steroid}$/C8*L*=O8 bonds.

4. Conclusions

Unlike lithocholic acid (1) which forms guest-free crystals by recrystallization from commonly used organic solvents (Arora *et al.*, 1976), the molecular triad (5) consisting of two lithocholic acid moieties linked by terephthalic acid packs more efficiently with pyridine molecules as guests. An expanded form of the infinite one-dimensional polymer seen in (5)·2Py is sustained by strong N—H···O hydrogen bonds and by pairwise $\pi\cdots\pi$ interactions between pyridine rings which are mutually antiparallel. Although deprived of the ability to form hydrogen-bonded double layer arrangements characteristic for bile acids, the investigated steroidal triads pack in a fashion resembling the chiral sheet arrangement of bile acids. The spacer fragments are invariably positioned in places occupied by the guest molecules in the bile acid clathrates. This suggests that the molecular shape and hydrophobic interactions, not the hydrogen bonds, play the decisive role in packing of steroids. Inclusion properties of the investigated triads might be controlled by the choice of the appropriate spacer and side chain functionality.

Financial support of the work (RJ, ZP) by the Polish Ministry of Science and Higher Education (Project No. 3T09A 085 28) is gratefully acknowledged.

References

Aakeröy, Ch. B., Desper, J., Leonard, B. & Urbina, J. F. (2005). *Cryst. Growth Des.* **5**, 865–873.
Aakeröy, Ch. B., Hussain, I., Forbes, S. & Desper, J. (2007). *CrystEngComm*, **9**, 46–54.
Allen, F. H. (2002). *Acta Cryst.* B**58**, 380–388.
Arora, S. K., Germain, G. & Declercq, J. P. (1976). *Acta Cryst.* B**32**, 415–419.
Babu, N. J. & Nangia, A. (2006). *Cryst. Growth Des.* **6**, 1995–1999.
Bhattarai, K. M., Davis, A. P., Perry, J. J., Walter, C. J., Menzer, S. & Williams, D. J. (1997). *J. Org. Chem.* **62**, 8463–8473.
Bonar-Law, R. P., Davis, A. P. & Dorgan, B. J. (1993). *Tetrahedron*, **49**, 9855–9866.
Bonar-Law, R. P. & Davis, A. P. (1993*a*). *Tetrahedron*, **49**, 9845–9854.
Bonar-Law, R. P. & Davis, A. P. (1993*b*). *Tetrahedron*, **49**, 9829–9844.
Bruno, I. J., Cole, J. C., Edgington, P. R., Kessler, M., Macrae, C. F., McCabe, P., Pearson, J. & Taylor, R. (2002). *Acta Cryst.* B**58**, 389–397.
Davis, A. P. (1993). *Chem. Soc. Rev.* **22**, 243–253.
Dayal, B., Speck, J., Bagan, E., Tint, G. S. & Salen, G. (1981). *Steroids*, **37**, 239–243.
De Riccardis, F., Di Filippo, M., Garrisi, D., Izzo, I., Mancin, F., Pasquato, L., Scrimin, P. & Tecilla, P. (2002). *Chem. Commun.* pp. 3066–3067.
Di Filippo, M., Izzo, I., Savignano, L., Tecilla, P. & De Riccardis, F. (2003). *Tetrahedron*, **59**, 1711–1717.
Duax, W. L. & Norton, D. A. (1975). *Atlas of Steroid Structure.* New York, Washington, London: IFI/Plenum.
Evans, S. M., Burrows, C. J. & Venanzi, C. A. (1995). *J. Mol. Struct. (Theochem.)* **334**, 193–205.
Gawroński, J. & Kacprzak, K. (2002). *Chirality*, **14**, 689–702.
Giglio, E. (1984). *Inclusion Compounds of Deoxycholic Acid*, edited by J. L. Atwood, J. E. D. Davies & D. D. McNicol, Vol. 2, pp. 207–229. London: Academic Press.
Giglio, E. & Quagliata, C. (1975). *Acta Cryst.* B**31**, 743–746.
Goto, C., Yamamura, M., Satake, A. & Kobuke, Y. (2001). *J. Am. Chem. Soc.* **123**, 12152–12159.
Gouin, S. & Zhu, X. X. (1998). *Langmuir*, **14**, 4025–4029.
Guthrie, J. P., Cossar, J. & Dawson, B. A. (1986). *Can. J. Chem.* **64**, 2456–2469.
Hishikawa, Y., Watanabe, R., Sada, K. & Miyata, M. (1998). *Chirality*, **10**, 600–618.
Hoffmann, S. & Kumpf, W. (1986). *Z. Chem.* **26**, 293–295.
Joachimiak, R. & Paryzek, Z. (2004). *J. Inclusin Phenom. Mol. Macromol. Chem.* **49**, 127–132.
Kobuke, Y. & Nagatani, T. (2001). *J. Org. Chem.* **66**, 5094–5101.
Kuma Diffraction (1995). *DATAPROC*, Version 9. Wrocław, Poland.
Li, Y. & Dias, J. R. (1997*a*). *Chem. Rev.* **97**, 283–304.
Li, Y. & Dias, J. R. (1997*b*). *Synthesis*, pp. 425–430.
Miyata, M. & Sada, K. (1996). *Comprehensive Supramolecular Chemistry*, edited by J. L. Atwood, J. E. D. Davis, D. D. McNicol & F. Vögtle, Vol. 6, pp. 147–176. Oxford: Elsevier Science.
Nahar, L. & Turner, A. B. (2003). *Steroids*, **68**, 1157–1161.
Nowak, E., Gdaniec, M. & Połoński, T. (2000). *J. Inclusion Phenom. Macromol. Chem.* **37**, 155–169.
Oxford Diffraction (2001*a*). *CrysAlis CCD*, Version 1.168. Oxford Diffraction, Oxfordshire, England.
Oxford Diffraction (2001*b*). *CrysAlisRed*, Version 1.168. Oxford Diffraction, Oxfordshire, England.
Oxford Diffraction (2004*a*). *CrysAlis CCD*, Version 1.171. Oxford Diffraction, Oxfordshire, England.
Oxford Diffraction (2004*b*). *CrystAlisRed*, Version 1.171. Oxford Diffraction, Oxfordshire, England.
Paryzek, Z., Koenig, H. & Tabaczka, B. (2003). *Synthesis*, pp. 2023–2026.
Pettit, G. R., Inoue, M., Kamano, Y., Dufresne, C., Christie, N., Niven, M. L. & Herald, D. L. (1988). *Chem. Commun.* pp. 865–867.

Pettit, G. R., Kamano, Y., Dufresne, C., Inoue, M., Christie, N., Schmidt, M. & Doubek, D. L. (1989). *Can. J. Chem.* **67**, 1509–1513.
Rychlewska, U. & Warżajtis, B. (2000). *Acta Cryst.* B**56**, 833–848.
Salunke, D. B., Hazra, B. G., Pore, V. S., Bhat, M. K., Nahar, P. B. & Deshpande, M. V. (2004). *J. Med. Chem.* **47**, 1591–1594.
Sheldrick, G. M. (1990). *Acta Cryst.* A**46**, 467–473.
Sheldrick, G. M. (2008). *Acta Cryst.* A**64**, 112–122.
Siemens (1989). *Stereochemical Workstation Operation Manual*, Release 3.4. Siemens Analytical X-ray Instruments, Inc., Madison, Wisconsin, USA.
Tamminen, J. & Kolehmainen, E. (2001). *Molecules*, **6**, 21–46.
Virtanen, E., Nissinen, M., Suontamo, R., Tamminen, J. & Kolehmainen, E. (2003). *J. Mol. Struct.* **649**, 207–218.
Vishweshwar, P., Nangia, A. & Lynch, V. M. (2002). *J. Org. Chem.* **67**, 556–565.
Xia, A., Selegue, J. P., Carrillo, A., Patrick, B. O., Parkin, S. & Brock, C. P. (2001). *Acta Cryst.* B**57**, 507–516.
Yoshimura, T., Hasegawa, S., Hirashima, N., Nakanishi, M. & Ohwada, T. (2001). *Bioorg. Med. Chem. Lett.* **11**, 2897–2901.